Plasma Diagnostics Using K_α Satellite Emission Spectroscopy in Light Ion Beam Fusion Experiments

J.J. MacFarlane, P. Wang,
J.E. Bailey, T.A. Mehlhorn, R.J. Dukart

January 1994

UWFDM-941

Submitted for publication to *Lasers and Particle Beams* as part of the 6th International Workshop on Atomic Physics for Ion Driven Fusion, 8–12 November 1993, Santa Fe NM.

FUSION TECHNOLOGY INSTITUTE

UNIVERSITY OF WISCONSIN

MADISON WISCONSIN

Plasma Diagnostics Using K_α Satellite Emission Spectroscopy in Light Ion Beam Fusion Experiments

J. J. MacFarlane and P. Wang

Fusion Technology Institute
University of Wisconsin
Madison, WI 53706

J. E. Bailey, T. A. Mehlhorn, and R. J. Dukart

Sandia National Laboratories
Albuquerque, NM 87185

January 1994

UWFDM-941

Submitted for publication to Lasers and Particle Beams as part of the 6th International Workshop on Atomic Physics for Ion Driven Fusion.

Abstract

K_α satellite spectroscopy can be a valuable technique for diagnosing conditions in high energy density plasmas. K_α emission lines are produced in intense light ion beam-plasma interaction experiments as $2p$ electrons fill partially open $1s$ shells created by the ion beam. In this paper, we present results from collisional-radiative equilibrium (CRE) calculations which show how K_α emission spectroscopy can be used to determine target plasma conditions in intense lithium beam experiments on Particle Beam Fusion Accelerator-II (PBFA-II) at Sandia National Laboratories. In these experiments, 8-10 MeV lithium beams with intensities of 1-2 TW/cm^2 irradiate planar multilayer targets containing a thin Al tracer. K_α emission spectra are measured using a x-ray crystal spectrometer with a resolution of $\lambda/\Delta\lambda \simeq 1200$. The spectra are analyzed using a CRE model in which multilevel ($N_L \sim 10^3$) statistical equilibrium equations are solved self-consistently with the radiation field and beam properties to determine atomic level populations. Atomic level-dependent fluorescence yields and ion-impact ionization cross sections are used in computing the emission spectra. We present results showing the sensitivity of the K_α emission spectrum to temperature and density of the Al tracer. We also discuss the dependence of measured spectra on the x-ray crystal spectral resolution, and how additional diagnostic information could be obtained using multiple tracers of similar atomic number.

1. Introduction

K_α spectroscopy can be a valuable technique for determining plasma conditions in high-intensity beam-plasma interaction experiments (Nardi & Zinamon 1981). K_α lines result from $2p \leftrightarrow 1s$ transitions. Thus, K_α absorption lines can be seen in the presence of an x-ray backlighter when ions have at least one vacancy in the $2p$ shell. K_α emission lines are produced by ions which have vacancies in the $1s$ shell and have at least one electron in the $2p$ shell. Absorption spectroscopy of inner shell transitions has been used in laser-produced plasma experiments to diagnose pusher conditions in inertial confinement fusion (ICF) target implosions (Hauer et al. 1986), to determine temperatures and densities in layered targets (Chenais-Popovics et al. 1989; Bruneau et al. 1990), and to measure opacities (Foster et al. 1991; Perry et al. 1991; Springer et al. 1992). K_α emission lines have been observed in several types of experiments, including high-temperature tokamak plasmas (Beiersdorfer et al. 1993) and beam-target interactions (Knudson et al. 1971; Watson et al. 1983). K_α emission spectroscopy has also recently been shown to be an important diagnostic technique in plasmas created by intense light ion beams (Bailey et al. 1990, 1994). Measuring x-ray lines is a particularly valuable approach in such experiments because it allows one to probe the interior regions of targets by looking in a spectral region where opacity effects are reduced.

Bailey et al. (1990) reported the first spectroscopic measurements of K_α x-ray satellites in an intense light ion beam experiment. The emission spectra were obtained during Particle Beam Fusion Accelerator-II (PBFA-II) proton beam experiments at Sandia National Laboratories. K_α emission spectra have also recently been observed in intense Li-beam experiments on PBFA-II (Bailey et al. 1994). In these experiments, plasmas temperatures of 30 to 50 eV were achieved (Bailey et al. 1994; MacFarlane et al. 1993, 1994). K_α emission lines are produced as the ion beam ejects K-shell electrons, which are subsequently filled by $2p$ electrons. Similarly, K_β lines can be produced by $3p \rightarrow 1s$ transitions. The K_α lines from He-like to Ne-like ions exhibit small but detectable shifts to shorter wavelengths due to reduced screening effects in the partially filled L-shell. Thus, K_α satellite spectra provide a measure of the ionization distribution of the target plasma. In addition, the intensity ratios from individual K_α lines can be used to determine plasma conditions (MacFarlane et al. 1994).

The purpose of this paper is to show how K_α satellite spectroscopy can be used to diagnose conditions in Li beam-heated plasmas. Results from detailed radiative and atomic physics calculations are presented for Al tracers at plasma conditions typical of

those achieved in recent PBFA-II experiments. In addition, to assess the reliability of our models, we compare results of a calculated Al K_α absorption spectrum with one measured in a laser-produced plasma experiment (Perry et al. 1991).

The outline of this paper is as follows. In Section 2, we describe the CRE and atomic physics models used to compute the K_α satellite spectra. Results are presented in Section 3, where we discuss the sensitivity of emission spectra to target plasma temperature, density, and atomic number. We also discuss the sensitivity of spectra to the crystal spectral resolution. A summary of this investigation is presented in Section 4.

2. Theoretical Models

Atomic level populations are computed by solving multilevel statistical equations self-consistently with the radiation field and ion beam properties (MacFarlane and Wang 1992). Processes considered in the statistical equilibirium equations are: collisional (electron impact) excitation, deexcitation, ionization, and recombination; photoexcitation, spontaneous and stimulated emission; photoionization, radiative and dielectronic recombination; ion beam-impact ionization of K-shell and L-shell electrons; and Auger ionization. Collisional coupling between states is "complete" in the sense that for each ion all non-autoionizing states are collisionally coupled together, as are all autoionizing levels. Coupling between non-autoionizing and autoionizing levels takes place via ion-impact ionization, Auger ionization, and spontaneous decay. Radiative coupling between levels is modeled for all transitions with oscillator strengths greater than 10^{-5}. This level of detail allows one to accurately track transitions into, out of, and between autoionizing levels, which becomes necessary when using the intensity ratios of individual lines as temperature and density diagnostics.

In our calculations for Al, we consider a total of 1266 atomic energy levels distributed over all 14 ionization stages. Roughly 60% of these are autoionizing levels, of which approximately 500 have M-shell spectators. Thus, K_β lines and K_α lines with M-shell spectator electrons were considered. Energy levels and oscillator strengths were calculated using a configuration interaction (CI) model with Hartree-Fock wavefunctions (Wang 1991; Wang et al. 1993a). The line spectrum is treated in intermediate coupling. Electron-impact collision data were computed using a combination of distorted wave, Coulomb-Born, and semi-classical impact parameter models. For forbidden transitions, distorted wave calculations were performed.

Radiation transfer effects were calculated using an escape probability model (Apruzese et al. 1980). Radiative processes do not significantly affect the level populations for Al at relatively high densities and low temperatures ($n \gtrsim 10^{20}\,\mathrm{cm}^{-3}$, $T \lesssim 40\,\mathrm{eV}$) as the plasma is collisionally dominated and the plasma populations are close to LTE. Opacity due to resonant self-absorption, however, can significantly impact the spectrum. Bound-bound, bound-free (including inner-shell), and free-free transitions are considered in the spectral calculations. Voigt profiles are assumed for the lines. Line widths include contributions from natural, Auger, Doppler, and Stark broadening.

Autoionizing levels in our model are populated as the beam ejects K-shell and, in the case of multiple ionization, L-shell electrons. The ion beam-impact ionization rate is:

$$R_{ii^*} = n_i\,\sigma_B(E_B)\,J_B\,,$$

where J_B and E_B are the current density (particle flux) and energy per particle of the beam, σ_B is the ion-impact ionization cross section, and n_i is the number density of target ions in level i. The indices i^* and i refer to the autoionizing state and the initial state (prior to K-shell ejection), respectively. In the CRE calculations, the Li beam is assumed to be fully ionized, monoenergetic, and spatially uniform. It is worth noting that the plasma is heated primarily by the interaction of the beam with outer shell (L-shell and M-shell) electrons. The ejection of K-shell electrons serves mainly as a diagnostic.

Multiple ionization processes are important in the PBFA-II Li beam experiments in that they do influence K_α emission spectra (see Section 3). To illustrate this, consider the case of an F-like ion in its ground state configuration. As a Li ion interacts with a target ion, several reactions are possible, including:

$$1s^2 2s^2 2p^5 \rightarrow \begin{cases} 1s^1 2s^2 2p^5 & \text{(single ionization)} \\ 1s^1 2s^2 2p^4 & \text{(double ionization)} \\ 1s^1 2s^1 2p^4 & \text{(triple ionization)}\,. \end{cases}$$

That is, for multiply charged ion beams the target ion can be stripped of more that one electron due to its interaction with a single projectile (Hill et al. 1976). Li beam-impact ionization cross sections for ground and excited states of Al were computed using a modified plane wave Born model (Madison & Merzbacher 1975; Brandt & Lapicki 1981), with corrections for Coulomb-deflection, perturbations of the target ion wavefunctions induced by the projectile, and relativistic effects on the target ion wavefunctions. This

model has been shown to more accurately predict cross sections at relatively low ion projectile energies than a plane-wave Born approximation model without correction terms (Brandt & Lapicki 1981; Wang et al. 1994).

In addition to ion beam-impact ionization, emission line intensities are dependent on the fluorescence yields. Fluorescence yields and Auger rates were calculated for each autoionizing level using an L-S coupling formalism with Hartree-Fock wavefunctions. The fluorescence rate (i.e., the rate at which K_α photons are emitted) from level i^* to level j is given by

$$R_{i^*j} = n_{i^*} A_{i^*j} ,$$

where A_{i^*j} is the spontaneous decay rate. The Auger rate can be expressed as

$$R_{i^*\kappa} = n_{i^*} [Y_{i^*}^{-1} - 1] \sum_j A_{i^*j} ,$$

where Y_{i^*} is the fluorescence yield of the autoionizing level i^*, and the index κ refers to the ground state of the next higher ionization stage.

3. Results

To test the reliability of our physics models in the K_α spectral region, we compare results of a calculated K_α satellite absorption spectrum with a spectrum measured for Al in a laser-produced plasma experiment at Lawrence Livermore National Laboratory (Perry et al. 1991). Figure 1 compares the calculated and experimental spectra. The plasma parameters in the calculations were taken to be those values determined from independent diagnostics in the experiment: $T = 58$ eV and $\rho = 0.02$ g/cm^3. The thickness of the plasma was 6.75 μm, which corresponds to a pre-expansion (solid density) foil thickness of 500 Å. Local thermodynamic equilibrium (LTE) populations were assumed in this particular calculation, as had been done in earlier analyses of these experiments (Abdahlah et al. 1991, Perry et al. 1991). Instrumental broadening was included by convolving the computed spectrum with a 0.6 FWHM Gaussian.

In Figure 1 the lines from He-like (He_α) and Li-like Al (labelled mn through kj; for nomenclature, see Boiko et al. (1978)) are individually identified. The He_α line is of course a $1s^2\,{}^1S \rightarrow 1s^1 2p^1\,{}^1P^0$ transition, while the Li-like satellites are $1s^2 2s^1 \rightarrow 1s^1 2s^1 2p^1$ and $1s^2 2p^1 \rightarrow 1s^1 2p^2$ transitions. Also shown in Figure 1 are Be-like (λ = 7.89-7.98 Å) and B-like (λ = 7.98-8.07 Å) satellites. The calculated spectrum is seen to be in good agreement with the experimental spectrum. Differences between the calculated and

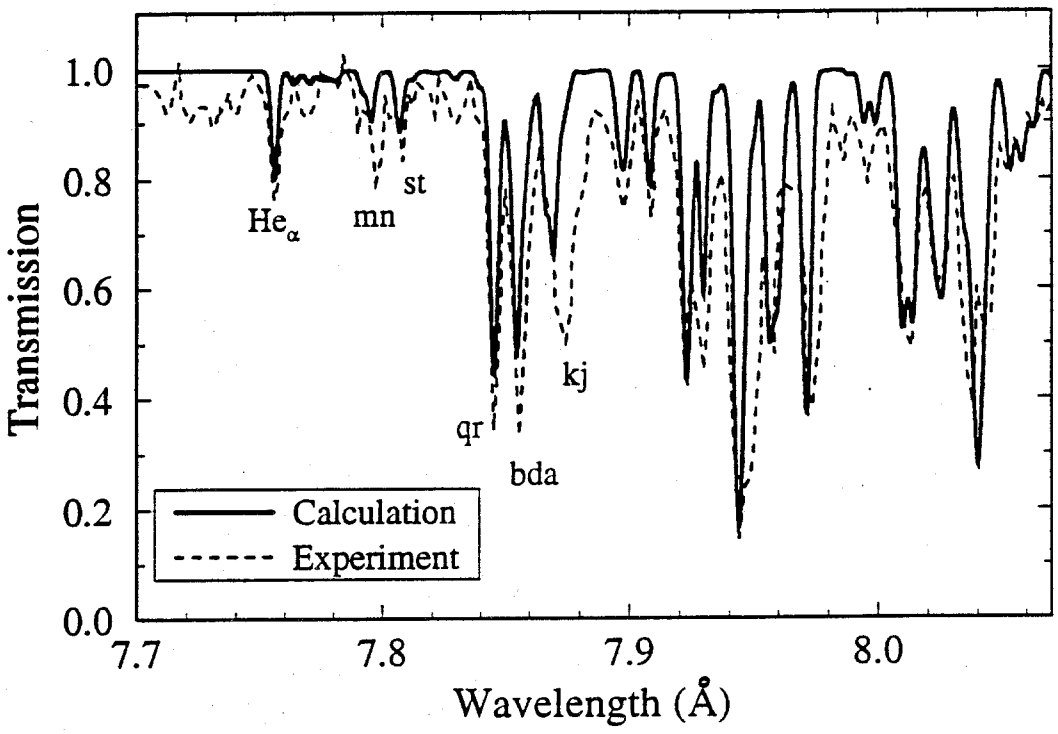

Figure 1. Comparison of calculated (solid curve) and experimental (dotted curve) K_α satellite absorption spectra for Al. Absorption features from He-like (He_α), Li-like (labelled *mn* through *kj*), Be-like (λ = 7.89-7.98 Å), and B-like (λ = 7.98-8.07 Å) aluminum are clearly seen.

experimental wavelengths are generally $\lesssim 3$ mÅ. In addition, we compared our calculated wavelengths and oscillator strengths for several transitions with other calculations (Chen and Iglesias 1993) and found good agreement. Probably the most noticeable discrepancy between our calculation and experiment occurs at the feature near $\lambda = 7.87$ Å, where the experimental absorption is both stronger and broader than in the calculations. This feature is a blend of the Li-like *kj* transitions ($1s^2 2p^1\,{}^2P \rightarrow 1s^1 2p^2\,{}^2D$) and Be-like transitions ($1s^2 2s^1 2p^1\,{}^3P \rightarrow 1s^1 2s^1 2p^2\,{}^3P$) . The reason for this discrepancy is not known at this time. Despite this, we consider the overall agreement between our calculation and the experimental spectrum to be reasonably good.

We now turn our attention to K_α satellite *emission* spectra, which are readily observed in intense light ion beam experiments because of the ability of the beam ions to create K-shell vacancies. Here, we consider multilayer planar targets with a 2000 Å-

thick Al tracer layer, which expands as it is heated to tens of eV (see Fig. 2). Targets of this type have recently been used in PBFA-II Li-beam experiments (Bailey et al. 1994). Similar targets, though with lower-Z tracers (F and Na), are also expected to be used in upcoming KALIF experiments at Kernforschungszentrum Karlsruhe (Goel et al. 1993). In all calculations described below, we assume the tracer region to be of uniform temperature and density. It is also assumed that the Li ion beam is spatially uniform and monoenergetic. We take the Li beam to be fully ionized, with an energy of 9 MeV per Li^{3+} ion. Unless indicated otherwise, the plotted spectra include instrumental broadening with $\lambda/\Delta\lambda = 1200$, which is consistent with the resolution obtained in recent PBFA-II experiments (Bailey et al. 1990, 1994).

The temperature-dependence of the emission spectrum is shown in Figure 3, where the He-like through B-like K_α satellites for Al are shown for temperatures ranging from 37 to 46 eV. In each case the ion density was 10^{20} cm^{-3} and the plasma thickness was 120 μm (i.e., equivalent to a 2000 Å-thick tracer which has expanded by a factor of 600). At 37 eV, the Be-like satellites are strongest. Note the structure of the Be-like satellites as compared to the absorption spectrum in Figure 1. In each case the feature near 7.945 Å, which is due to a combination of ($1s^1 2s^1 2p^2\,{}^3P \rightarrow 1s^2 2s^1 2p^1\,{}^3P$) and ($1s^1 2s^1 2p^2\,{}^3D \rightarrow 1s^2 2s^1 2p^1\,{}^3P$) transitions, is strongest. Above 40 eV, the Li-like and He-like lines exhibit the greatest intensities. The maximum intensities attained by these satellites can be considerably stronger than those of lower ionization stages because of their relatively high fluorescence yields (Wang et al. 1993a), which is of course unity for He_α because the upper state ($1s^1 2p^1\,{}^1P^0$) is not an autoionizing state. Note that the sensitivity of the satellite spectrum to small changes in temperature is quite good. In particular, note the strength of the He_α line to Li-like satellites and the relative strengths of the Be-like satellites. In addition, this is a particularly good temperature region for using Al as a diagnostic because of the less complex atomic physics for these few electron systems.

Note that even for the He_α line, the main mechanism for the populating upper states of the fluorescing transitions in this temperature regime is ion beam-impact ionization. That is, electron impact excitation from low lying states is unimportant, as is dielectronic recombination (Wang et al. 1993b). There is, however, some redistribution of the autoionization state populations due to transitions with other autoionizing states. In fact, these latter processes can lead to important density diagnostics from K_α satellite line intensity ratios (MacFarlane et al. 1994).

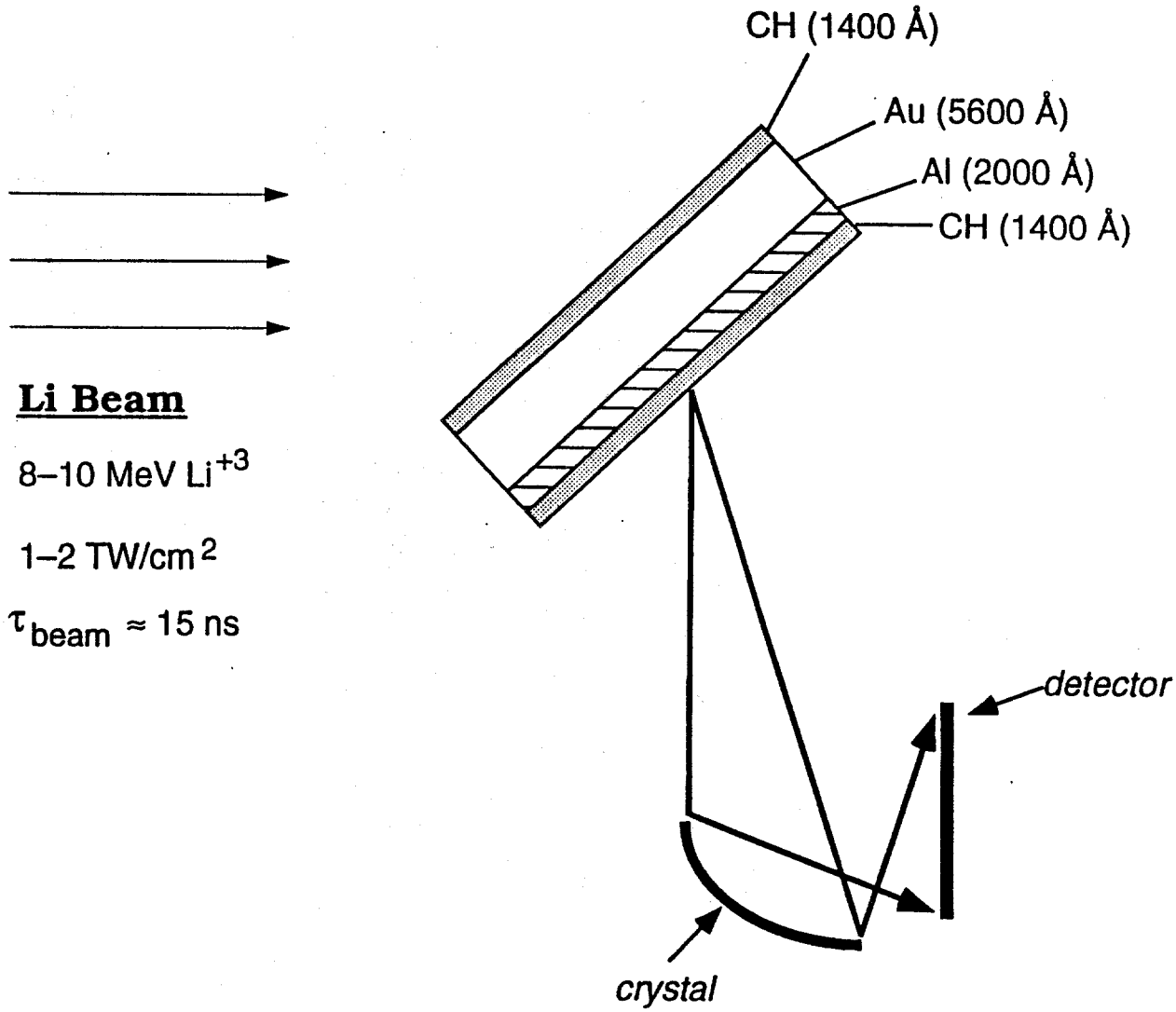

Figure 2. Schematic of planar multilayer targets used in PBFA-II Li beam experiments.

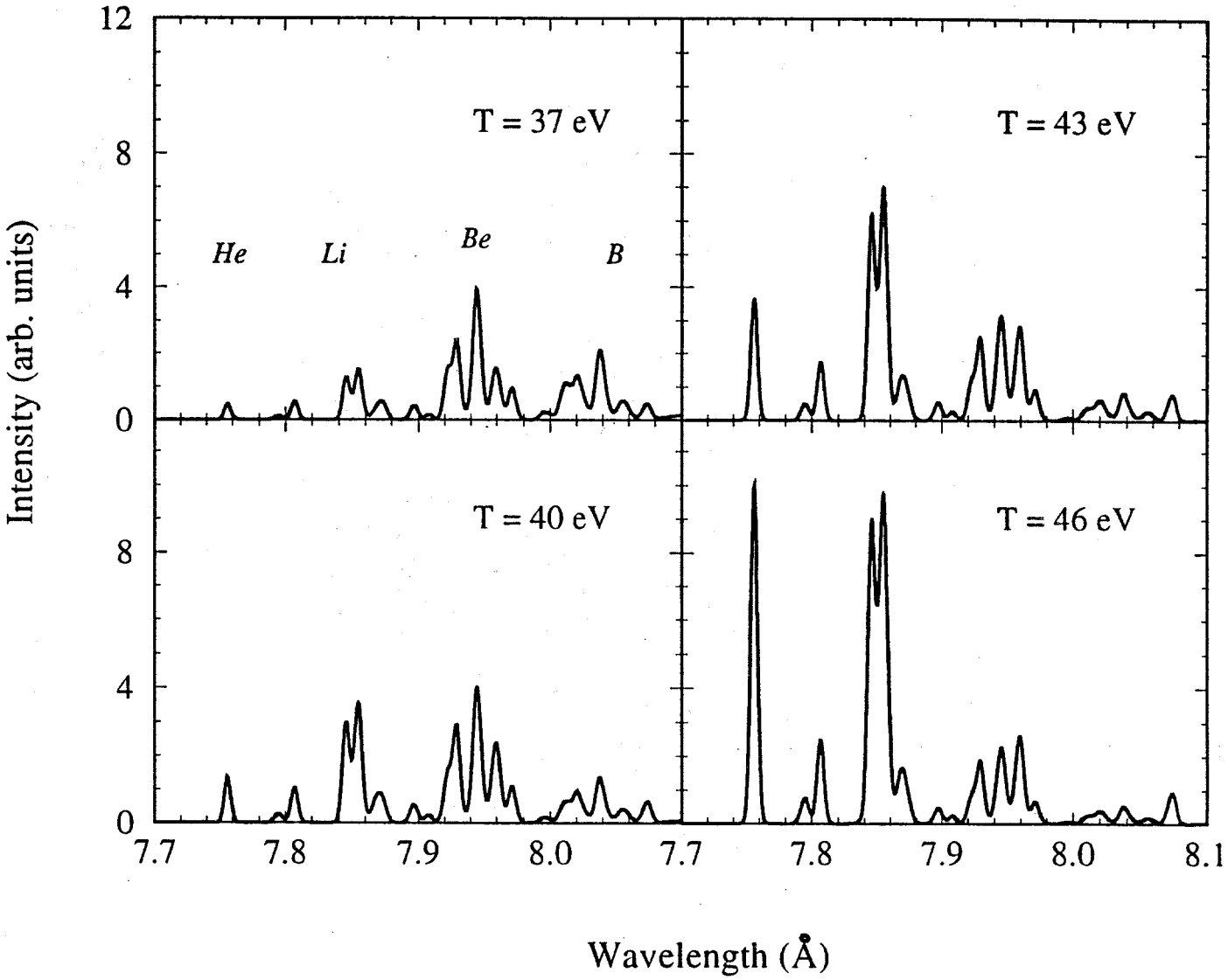

Figure 3. Dependence of calculated K_α satellite emission spectra on temperature. In each case the ion density was 10^{20} cm^{-3} and plasma thickness was 120 μm.

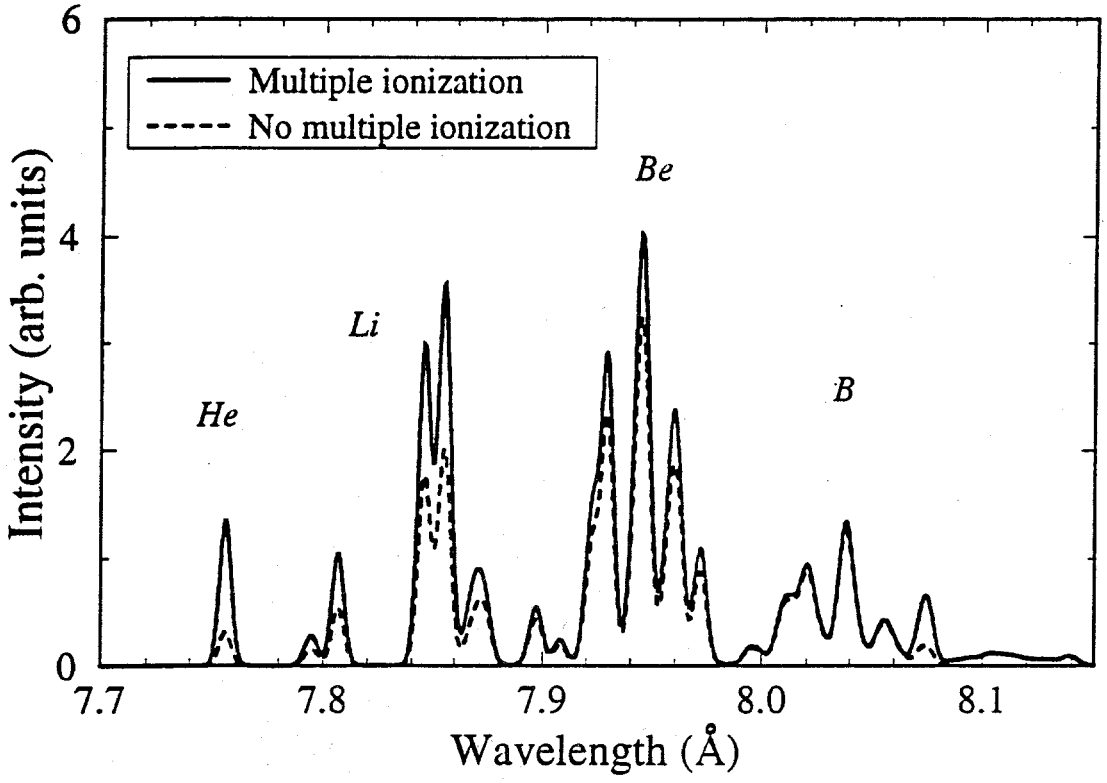

Figure 4. Calculated K_α emission spectra for a Li beam-heated Al plasma at $T = 40$ eV, $n = 10^{20}$ ions/cm^3, and $L = 120\,\mu$m. The influence of multiple ionization by the Li beam can be seen by comparing the results computed with (solid curve) and without (dotted curve) multiple ionization.

Multiple ionization processes — that is, the simultaneous ejection of one or more L-shell electrons along with a K-shell electron — can be important in intense Li beam experiments on PBFA-II. Cross sections for multiple ionization tend to be significantly larger for lower ionization stages of the target plasma because of reduced binding effects. Nevertheless, these processes can still be important for the relatively high ionization stages of Al. This is shown in Figure 4, where the results of two calculations are shown: one in which multiple ionization processes were included, and one in which only single ionization (i.e., K-shell) events were considered. Other than that, the plasma and ion beam conditions were identical in the two calculations. Figure 4 shows that when multiple ionization is ignored, the He_α line is reduced by roughly a factor of 4, while the Li-like features are reduced by about a factor of 2. The former occurs because the $1s^1 2p^1$

configuration of He is being populated not only via single ionization from Li-like Al ($1s^2 2p^1 \rightarrow 1s^1 2p^1$), but also by double ionization from Be-like Al ($1s^2 2s^1 2p^1 \rightarrow 1s^1 2p^1$ and $1s^2 2p^2 \rightarrow 1s^1 2p^1$). This occurs despite the fact that the double ionization cross sections are smaller by about an order of magnitude (Wang et al. 1994). The smaller cross section is compensated for by the ionization fraction of Be-like Al ($f_{\rm Be} = 0.067$ in this case) being much higher than that of Li-like Al ($f_{\rm Li} = 0.0021$). Multiple ionization is seen to be less important for Be- and B-like Al because these ions are closer to the peak in the ionization distribution at this temperature and density.

The sensitivity of the emission spectrum to density is shown in Figure 5. The most noticeable effect of moving to higher density is that the satellites from the higher ionization stages decrease significantly. This simply reflects the change in ionization of the bulk plasma due to 3-body recombination. It is also seen that the relative strengths of the Be-like features near 7.925 Å and 7.970 Å change markedly, with the shorter wavelength feature decreasing significantly as the density increases. A detailed description of line ratio diagnostics using K_α satellites will be presented elsewhere (MacFarlane et al. 1994).

Clearly, to get accurate measurements of the intensities of the K_α satellites, good spectral resolution is necessary. Figure 6 shows the influence of emission spectrum on the instrumental resolution. At a resolution of $\lambda/\Delta\lambda = 500$, the lines are broadened quite severely, and little structure is seen for, say, the Li-like and Be-like satellites. On the other hand, at resolutions $\gtrsim 2000$ the structure is quite clearly seen, with 5 strong features easily resolved for Be-like Al (as is seen in absorption in Figure 1). The dominant broadening mechanism in the spectrum is instrumental broadening. Intrinsic broadening for the K_α lines at these densities tends to be dominated by Auger processes. Stark broadening is relatively unimportant at these densities. It is important to be able to resolve this structure in intense light ion beam experiments as measurements of relative line intensities can provide valuable information for accurately determining target plasma conditions.

Finally, it is interesting to examine the K_α satellite spectra for tracer materials of similar atomic number. The K_α spectrum from a second tracer could provide additional constraints for determining target plasma conditions. In addition, placing two tracers at different locations in a target could allow for the study of temperature gradients in light ion beam-heated targets. Figure 7 shows the K_α spectrum computed for a 120 μm-thick, $n = 10^{20}$ ions/cm^3 Mg tracer at $T = 40$ and 46 eV. Note that these conditions are similar to those shown in Figure 3 for Al. At these temperatures the He_α line and

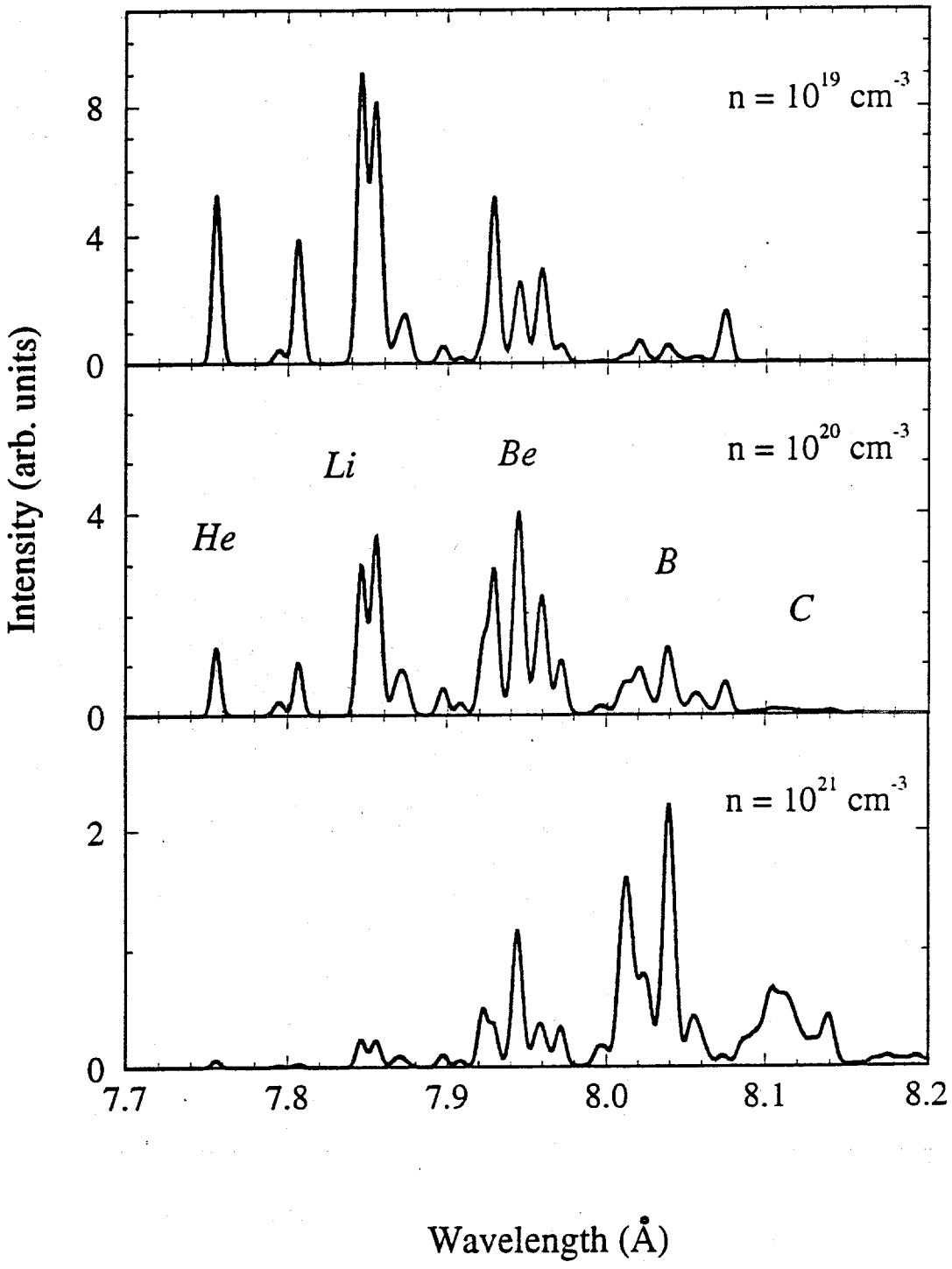

Figure 5. Density-dependence of Al K_α satellite spectrum. In each case, $T = 40$ eV and $L = 120\,\mu$m.

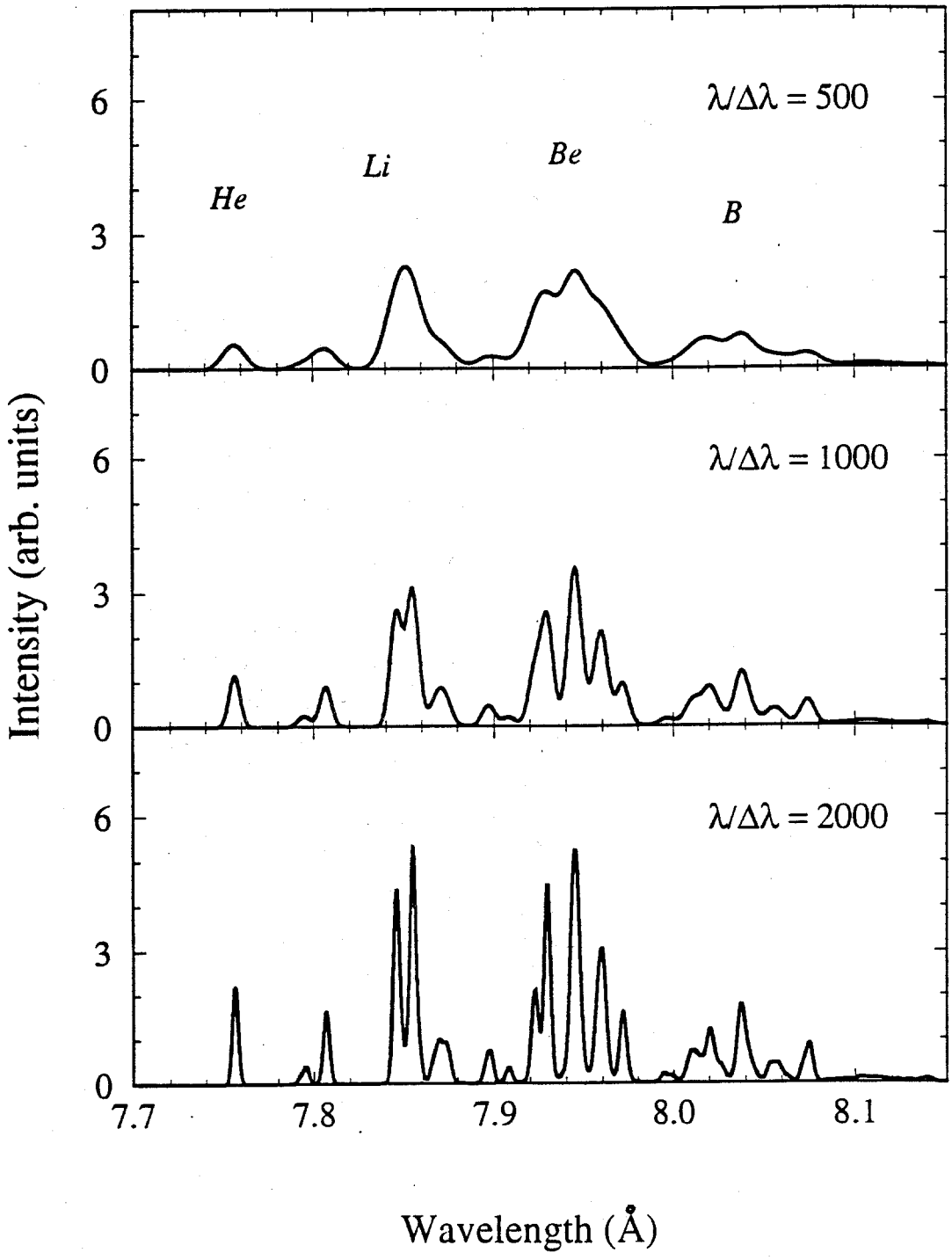

Figure 6. Dependence of K_α satellite emission spectrum on instrumental resolution. In each case, the plasma conditions are $T = 40$ eV, $n = 10^{20}$ ions/cm^3, and $L = 120\,\mu$m. Considerably more structure is seen as the resolution is increased from 500 to 2000.

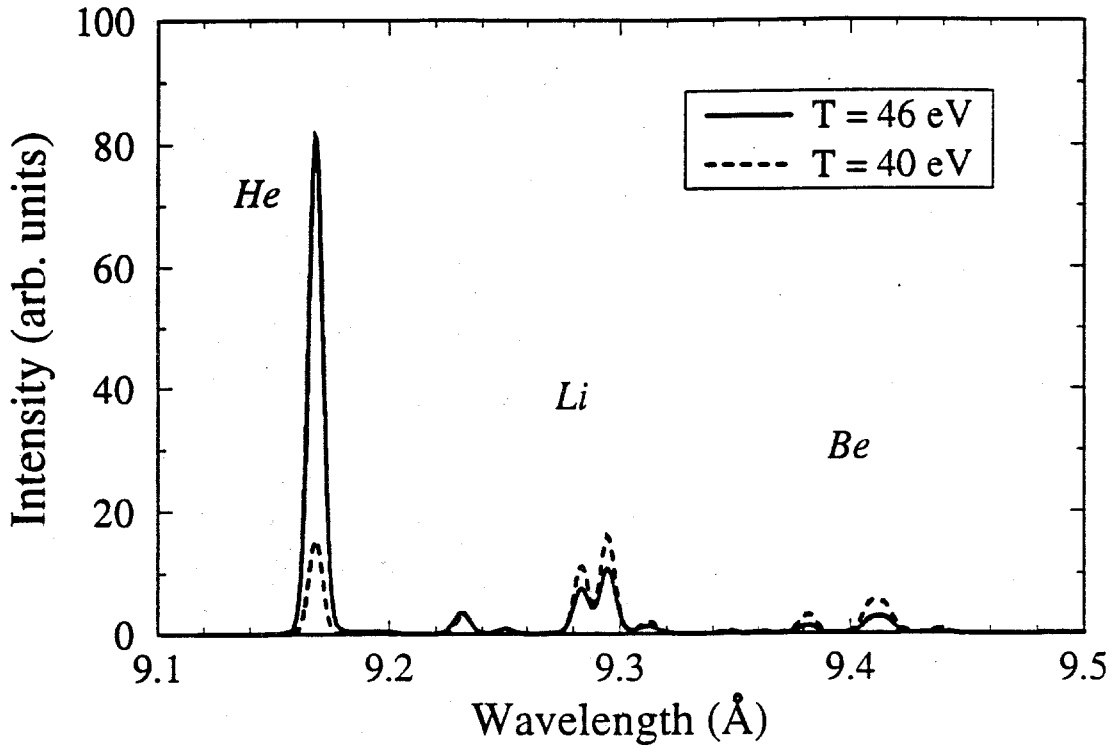

Figure 7. K_α satellite spectra calculated for a Mg tracer with $n = 10^{20}$ ions/cm^3, and $L = 120\,\mu$m.

Li-like satellites are predicted to have the strongest intensities. Figure 7 clearly shows the dramatic increase in the Mg He_α intensity with temperature. Again, the He_α intensity can be significantly higher because it is not depopulated by autoionizing processes. It is also much stronger than the Al He_α line for these conditions because of the lower relative ionization potentials for Mg. Note that while the ordinates are given as "arbitrary units", the units in Figures 3 through 7 are the same. Thus, the intensity of the Mg He_α line is predicted to be approximately 8 times greater than the Al He_α line at $T = 46$ eV. The use of multicomponent tracers will be pursued in future PBFA-II target experiments.

4. Summary

We have described how emission spectroscopy of the K_α satellite spectral regions of moderate-Z elements such as Al and Mg can be used to diagnose target plasma conditions in intense light ion beam-plasma interaction experiments. The sensitivity of the emission spectrum to both temperature and density were studied, as was the influence of instrumental broadening. In addition, it was shown that multiple ionization processes can impact the observed spectrum in PBFA-II Li beam-plasma interaction experiments. Future investigations will concentrate on using line intensity ratios from K_α transitions to determine target plasma conditions, as well as analyzing spectra obtained from targets with multicomponent tracers.

Acknowledgements

We wish to thank the entire PBFA II experimental group for their efforts. In addition, we gratefully acknowledge M. Chen and C. Iglesias for comparing results of their atomic physics calculations with ours. This work has been supported in part by the U.S. Department of Energy under Contract No. DE-AC04-94AL85000, and by Kernforschungszentrum Karlsruhe (FRG) through Fusion Power Associates.

References

ABDALLAH, J., CLARK, R. E. H., & PEEK, J. M. 1991 *Phys. Rev. A* **44**, 4072.

APRUZESE, J. P., DAVIS, J., DUSTON, D. & WHITNEY, K. G. 1980 *J.Q.S.R.T.* **23**, 479.

BAILEY, J., CARLSON, A. L., CHANDLER, G., DERZON, M. S., DUKART, R. J., HAMMEL, B. A., JOHNSON, D. J., LOCKNER, T. R., MAENCHEN, J., MCGUIRE, E. J., MEHLHORN, T. A., NELSON, W. E., RUGGLES, L. E., STYGAR, W. A. & WENGER, D. F. 1990 *Lasers & Particle Beams* **8**, 555.

BAILEY, J. E. et al. 1994 in preparation.

BEIERSDORFER, P., PHILLIPS, T., JACOBS, V. L., HILL, K. W., BITTER, M., VON GOELER, S. & KAHN, S. M. 1993 *Astrophys. J.* **409**, 846.

BOIKO, V. A., FAENOV, A. Y., & PIKUZ, S. A. 1978 *J.Q.S.R.T.* **19**, 11.

BRANDT, W. & LAPICKI, G. 1981 *Phys. Rev. A* **23**, 1717.

BRUNEAU, J., CHENAIS-POPOVICS, C., DESENNE, D., GAUTHIER, J. C., GEINDRE, J. P., KLAPISCH, M., LE BRETON, J. P., LOUIS-JACQUET, M., NACCACHE, D. & PERRINE, J.-P. 1990 *Phys. Rev. Lett.* **65**, 1435.

CHEN, M. & IGLESIAS, C. 1993 private communication.

CHENAIS-POPOVICS, C., FIEVET, C., GEINDRE, J. P., GAUTHIER, J. C., LUC-KOENIG, E., WYART, J. F., PEPIN, H. & CHAKER, M. 1989 *Phys. Rev. A* **40**, 3194.

FOSTER, J. M., HOARTY, D. J., SMITH, C. C., ROSEN, P. A., DAVIDSON, S. J., ROSE, S. J., PERRY, T. S. & SERDUKE, F. J. D. 1991 *Phys. Rev. Lett.* **67**, 3255.

GOEL, B. et al. 1993 presented at the 6th International Workshop on Atomic Physics for Ion Driven Fusion, Santa Fe, NM.

HAUER, A., COWAN, R. D., YAAKOBI, B., BARNOUIN, O. & EPSTEIN, R. 1986 *Phys. Rev. A* **34**, 411.

HILL, K. W., DOYLE, B. L., SHAFROTH, S. M., MADISON, D. H. & DESLATTES, R. D. 1976 *Phys. Rev. A* **13**, 1334.

KNUDSON, A. R., NAGEL, D. J., BURKHALTER, P. G. & DUNNING, K. L. 1971 *Phys. Rev. Lett.* **26**, 1149.

MacFARLANE, J. J. & WANG, P. 1992 *Lasers & Particle Beams* **10**, 349. More details on CRE and atomic physics models are provided in University of Wisconsin Fusion Technology Institute Reports UWFDM-822 (1990), UWFDM-847 (1991), and UWFDM-873 (1992).

MacFARLANE, J. J., WANG, P., BAILEY, J., MEHLHORN, T. A., DUKART, R. J. & MANCINI, R. F. 1993 *Phys. Rev. E* **47**, 2748.

MacFARLANE, J. J. et al. 1994, in preparation.

MADISON, D. H. & MERZBACHER, E. 1975 in *Atomic Inner-Shell Processes, Vol. 1*, D. Craseman, ed. (Academic Press, New York).

NARDI, E. & ZINAMON, Z. 1981 *J. Appl. Phys.* **52**, 7075.

PERRY, T. S., DAVIDSON, S. J., SERDUKE, F. J. D., BACH, D. R., SMITH, C. C., FOSTER, J. M., DOYAS, R. J., WARD, R. A., IGLESIAS, C. A., ROGERS, F. J., ABDALLAH, J., STEWART, R. E., KILKENNY, J. D. & LEE, R. W. 1991 *Phys. Rev. Lett.* **67**, 3784.

SPRINGER, P. T., PERRY, T. S., FIELDS, D. F., GOLDSTEIN, W. H., WILSON, B. G. & STEWART, R. E. 1992 in *Atomic Processes in Plasmas, AIP Conference Proceedings 257*, E. S. Marmer and J. L. Terry, eds. (Amer. Inst. Phys., New York).

WANG, P. 1991 Ph.D. Dissertation, University of Wisconsin, Dept. of Nuclear Engr. & Engr. Physics, Madison, WI.

WANG, P., MACFARLANE, J. J. & MOSES, G. A. 1993a *Phys. Rev. E* **48**, 3934.

WANG, P., MACFARLANE, J. J. & MOSES, G. A. 1993b presented at the 6th International Workshop on Atomic Physics for Ion Driven Fusion, Santa Fe, NM.

WANG, P., MACFARLANE, J. J. & MOSES, G. A. 1994 this proceedings.

WATSON, R. L., BENKA, O., PARTHASARADHI, K., MAURER, R. J. & SANDERS, J. M. 1983 *J. Phys. B* **16**, 835.